A study of wind turbine power generation and turbine/tower interaction using large eddy simulation

R. J. A. Howard[†]

Departmento de Engenharia Mecânica, Universidade de Aveiro,
Campo Universitário de Santiago, 3810-193 Aveiro, Portugal

J. C. F. Pereira[‡]

Mechanical Engineering Department, LASEF, Instituto Superior Técnico,
Avenida Rovisco Païs, Lisbon 1049-001, Portugal

Abstract.   Wind turbines are highly complex structures for numerical flow simulation. They normally comprise of a turbine mounted on a tower thus the movement of the turbine blades and the blade/tower interaction must be captured. In addition the ground effect should also be included. There are many more important features of wind turbines and it is difficult to include all of them. A simplified set of features is chosen here for both the turbine and the tower to show how the method can begin to identify the main points connected with wind turbine wake generation and tip vortex tower interaction. An approach to modelling the rotating blades of a turbine is proposed here. The model uses point forces based on blade element theory to model the blades and takes into account their time dependent motion. This means that local instantaneous velocities can be used as a basis for the blade element theory. The model is incorporated into a large eddy simulation code and, although many important features are left out of the model, the velocity/power performance relation is generally of the correct order of magnitude. Suggested improvements to the method are discussed.

Keywords: wind turbines; wind turbine/tower interaction; wakes; large eddy simulation.

1. Introduction

Most wind farms currently in use contain a high density of wind turbines. For this reason it is important to understand how the wake behind one turbine can affect the flow and hence the power output of other turbines. Basic fluid structure fluctuation phenomena are presented with special relevance to the interaction of the turbine blade tip vortices with the turbine supporting tower structure. From the practical point of view this information is important to decide the orientation, size and power output of a wind farm.

Large eddy simulation is an approach which provides more information than classic one point closure turbulence modelling methods based on the stationary Navier-Stokes equations. In recent

† Corresponding Author, E-mail: rhoward@mec.ua.pt
‡ Professor, Head of LASEF Research Group, E-mail: jose@navier.ist.utl.pt

years LES has become a powerful tool for studying complex flows. There have been several different computational and experimental studies of wind turbines and Barthelmie (2002) shows the results of different groups who have examined wind turbine wakes in a project called Efficient Development of Offshore Windfarms (ENDOW). Calculations were compared with measurements made at an offshore site. All numerical approaches used steady state two-equation type turbulence modelling methods and simple models for the wind turbines. Steady state two-equation model calculations using the FLUENT software was also carried out by Hahm and Kröning (2001). The turbine model was more complicated and used a sliding grid mechanism between the domain for resolving the blades and the domain for resolving the wake. Blade element theory was used by Giguère and Selig (1999) and combined with flowfield effects derived from a momentum balance and Masson, *et al.* (2001) and Ammara, *et al.* (2002), modelled the blades as an actuator disk and included turbulence effects with a constant turbulent viscosity.

There have been other studies of the time dependent behaviour of wind turbines. Time dependent Reynolds averaged Navier-Stokes equations in which the computational domain rotated around a full three dimensional representation of the blades was performed by Xu and Sankar (2000). This study produced accurate results but required a large number of grid points. Since the domain was rotating the method cannot easily be applied to the problems studied here in which there is a complex ground plane. Sorensen and Shen (2002), carried out a study using a vorticity formulation of the Navier-Stokes equations and also obtained accurate results however their model was applied within a cylindrical polar coordinate system which cannot readily be incorporated into more complex system studied here.

Snel (1998) states: *up to date no non-stationary time-realistic 3D Navier-Stokes solutions for wind turbine blades have been reported.* Here we work towards such an approach with simplification of the turbine blade using blade element theory. Application of the turbine model is generalised so that the domain grid is not mapped around the turbine and the model can potentially be applied within any complex geometry domain.

The method is explained as follows: firstly some basic information about LES is provided with an explanation of how the model is applied for moving turbine blades. This is followed by some power curve validation, a study of the flowfield tip vortex and some analysis of the tower/blade
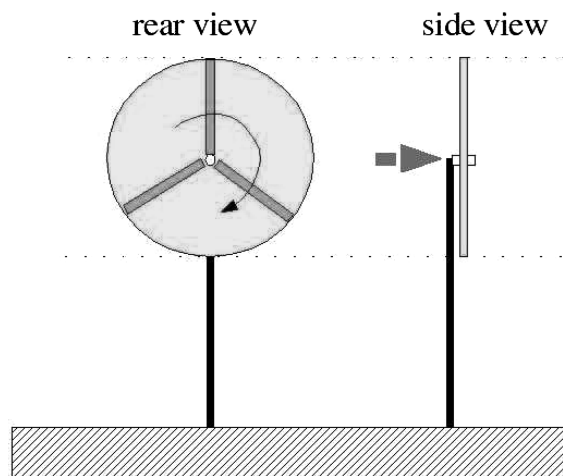
Fig. 1 A schematic diagram of a wind turbine with the blades positioned behind the tower

interaction. The paper ends with a discussion and a conclusion of the main points. The authors are unaware of any other LES numerical study aiming to investigate the wind turbine blade/tower interaction which also includes studies of the three-dimensional time dependent flow structures.

2. An approach to large eddy simulation on non-structured grids

In this study the code Trio-U, PRICELES is used. This code, written in c^{++}, is object oriented and is developed at the *Commissariat à l'Energie Atomique* in Grenoble, France to carry out thermohydraulic large eddy simulations of flow around complex geometries on parallel computers. The flexibility of the code makes it possible to make calculations on both structured and non-structured meshes however, as will be explained below, it is possible to carry out quite detailed wind turbine studies using the more rapid structured numerical method. Here the incompressible, time dependent, Navier-Stokes equations are solved. The system of equations solved is thus a momentum equation

$$\frac{\partial u_i}{\partial t} + u_j \frac{\partial u_i}{\partial x_j} = -\frac{1}{\rho}\frac{dp}{dx_i} + \frac{\partial}{\partial x_j}\left((v + v_t)\frac{\partial u_i}{\partial x_j}\right) \tag{1}$$

with continuity

$$\frac{\partial u_i}{\partial x_i} = 0 \tag{2}$$

These are the filtered or resolved Navier-Stokes equations (i.e. all variables are considered to be filtered or resolved so no additional notation is used). Turbulent motions that occur at scales smaller than the grid size are modelled using the subgrid model. The word "filtered" is used because, in effect, the flow is implicitly filtered at the grid scale. We can therefore say that the larger scale turbulent motions that can be captured by the grid are "resolved".

Second order central differences are used for the convection with 3rd order Runge-Kutta for time advancement. The time step size is chosen from limiting values of the convective and diffusive terms according to a Courant-Friedrich-Lewy (CFL) condition of 1. This led to time steps typically between $0.005s < \delta t < 0.07s$ depending on the inlet velocity. A preconditioned conjugate gradient method is used to solve the divergence condition for the pressure update. The subgrid model used to account for the small scales is the standard Smagorinsky model with a subgrid constant, $c_s = 0.2$. This constant was derived for homogeneous isotropic turbulence (see Sagaut 2004). Adjustments to the constant have been used in different studies. For more sensitivity a more advanced model should ultimately be used. Here it is considered a suitable starting point. The Smagorinsky turbulent eddy viscosity relation is $vt = (c_s\Delta)^2 S$ where Δ represents the local grid size and $S = \sqrt{2S_{ij}S_{ij}}$ the modulus of the strain rate invariant $S_{ij} = 0.5(\partial u_i/\partial x_j + \partial u_j/\partial x_i)$.

Ackermann (2000) has carried out some validation of the numerical method for turbulent flows. The code was also used by Howard and Pourquié (2002) to study large eddy simulation of a high Reynolds number simplified car body type complex geometry flow.

3. A wind turbine model for large eddy simulation

The model used here is based on blade element theory. There is quite a lot of literature available for further background on blade element theory. One quite accessible explanation is

Wood (2002) and there is a good description given by Jonkman (2003). A brief summary is provided here for completeness.

The aerodynamic characteristics of blade element theory are used to simplify the forces of the blade surface on the flow to point forces acting around the blade aerodynamic centre. Thus a wind turbine blade is simplified to a line of point forces each of which have the aerodynamical behaviour provided by blade element theory. The main difference between the approach here and the standard application of blade element theory is the way that the forces, f_i, are included on the right hand side of Eq. (1) of the large eddy simulation. In this study the locations of the points are made to rotate in the same way as the blades of the turbine and so the velocities used for the blade element theory vary locally in time and space. The purpose of this section is to explain the idea behind the model and how it is implemented.

$$\frac{\partial u_i}{\partial t} + u_j \frac{\partial u_i}{\partial x_j} = -\frac{1}{\rho}\frac{dp}{dx_i} + f_i + \frac{\partial}{\partial x_j}\left((\nu + \nu_t)\frac{\partial u_i}{\partial x_j}\right) \tag{3}$$

with continuity

$$\frac{\partial u_i}{\partial x_i} = 0 \tag{4}$$

The external body forcing term f_i (force per unit density) produced by the local thrust, δT, of a turbine blade is

$$f = \frac{\delta T}{\rho} \tag{5}$$

Blade element theory can be used to provide sufficient information to estimate the lift and drag forces on a blade element caused by the air. This can then be used to calculate the equal and opposite thrust force and torque the blade exerts on the air. Fig. 2 shows some of the key parameters used to calculate these forces. This figure shows the geometric pitch angle β and the induced pitch angle

$$\phi = \tan^{-1}\left(\frac{V_{axial}}{\omega r + V_{radial}}\right) \tag{6}$$

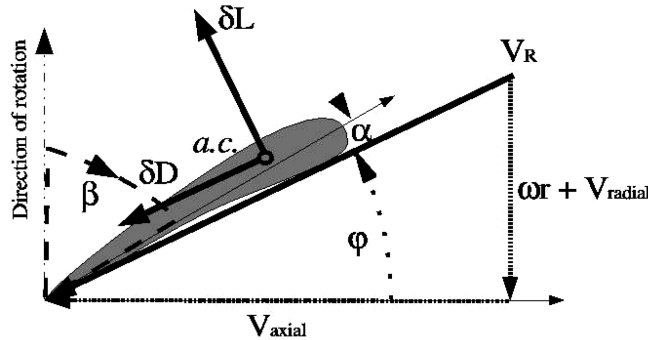due to the relative velocity V_R. This velocity in turn comes from the axial, V_{axial}, and radial,

Fig. 2 The forces, geometry and local flow orientation on a general blade element

$\omega r + V_{radial}$ components of the flow where $V_R = sqrt(V_{axial}^2 + (\omega r + V_{radial})^2)$. The local velocity of the flow in the radial direction is V_{radial} and the angular velocity of the blade element is ωr. The angle of attack of a blade element α is $\alpha = \phi - \beta$ and from two-dimensional aerofoil theory, the lift coefficient, c_L, can be obtained. In this case a simple approximation for the relationship between c_L and α is used. This is

$$c_L = c_{L0} + (c_{L(max)} - c_{L0})\sin(\pi\alpha/(2\alpha_{max})) \tag{7}$$

where c_{L0} is the lift coefficient when $\alpha = 0$, $c_{L(max)}$ is the maximum lift coefficient and α_{max} is the angle of attack for $c_L = c_{L(max)}$. At the inboard region near the blade root the angle of attack can become very large due to the low angular velocities. Here this problem is avoided by removing the inboard 15 percent of the blade from the power generating 7 and treating it as a force opposing the incoming flow velocity. For angles of attack greater than 20 degrees the c_L value is kept as a constant corresponding to the value with an angle of attack of 20 degrees. This treatment is not ideal and more appropriate modifications to blade element theory for rotating blades are indicated in the discussion and further work section.

The lift and drag forces act on the aerodynamic centre (*a.c.* on Fig. 2) of a given blade element and can be written as

$$\delta L = c(r)\delta r \frac{1}{2}\rho V_R^2 c_L \tag{8}$$

$$\delta D = c(r)\delta r \frac{1}{2}\rho V_R^2 c_D \tag{9}$$

where the local chord length $c(r)$ (a geometric property of a blade) is allowed to vary linearly along the radial length of the blade $\delta_c = c_{root}(1 - r/R) + c_{tip}r/R$ with given the root and tip chord values (c_{root} and c_{tip}).

These forces occur parallel and normal to the relative velocity V_R direction and thus lead to thrust T and torque Q components where

$$\delta T = \delta L\cos\phi + \delta D\sin\phi \tag{10}$$

and

$$\delta Q/r = \delta L\sin\phi - \delta D\cos\phi \tag{11}$$

Here it is assumed that, for a stalled wind turbine, the torque is zero. However, it is noted in the discussion and further work section that this approximation is not correct. The two relations are then combined

$$\delta T = \delta L(\cos\phi + \sin\phi\tan\phi) \tag{12}$$

and hence the local forcing (with the direction vector n_i) can be written as

$$f_i = c_L c(r)\delta r \frac{1}{2}V_R^2 (\cos\phi + \sin\phi\tan\phi)n_i \tag{13}$$

and the local power

$$p = V_{axial}c_L c(r)\delta r \frac{1}{2}V_R^2 (\cos\phi + \sin\phi\tan\phi) \tag{14}$$

so the total power at a given moment is

$$P = \sum_{N=1}^{Nb} \int_0^R p dr \qquad (15)$$

where Nb is the number of blades and R is the radius of the turbine or rather the length of a blade.

This model is different from the majority of other approaches discussed because the calculation is non-stationary and the blades are in rotation. Masson, *et al.* (2001) and Ammara, *et al.* (2002) discuss a way to describe a circular object on a cartesian mesh. The procedure involves using point forces to describe the dynamic interaction between the fluid and the blades and does not require a change in reference frame (such as between cylindrical polar coordinates and a cartesian frame). In this case there is no special treatment for the difference between the actual location of the point force within an element and the location of the element centres. Thus, the point forces are effectively applied at the element centres. This means that the surface where the forcing is applied varies as the blades rotate, more comments on this are given in the section on discussion and further work.

The performance of the model was compared with a standard one dimensional, stationary blade element approach used by Giguère and Selig (1999). The model was found to reproduce the same order of magnitude in the power production as that of Giguère and Selig (1999). For a complete comparison, experimental results for the power curve are required along with detailed information of the full geometric and aerodynamic properties of the turbine and its blades. Without the full experimental results for comparison it is not possible to draw concrete conclusions, however the model presented here does indicate some resolution dependence particularly at high velocities.

4. Results

The wind turbine analysed is based on a three bladed, twisted and tapered National Renewable Energy Laboratory, Combined Experimental Rotor, studied by Giguère and Selig (1999) (this paper will be referred to as G and S in the Figures). This wind turbine has a blade diameter of 10.064 metres and a rotational velocity of 71.63 revolutions per minute.

The blade geometry was chosen to be as close as possible to Giguère and Selig (1999). Fig. 3 shows the taper and twist distributions used. Fig. 4 shows the lift curve slope for the aerofoil
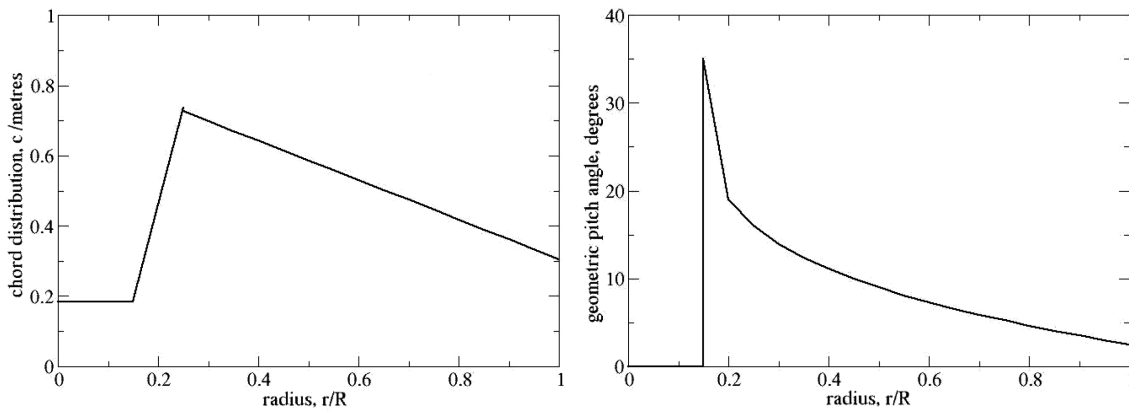

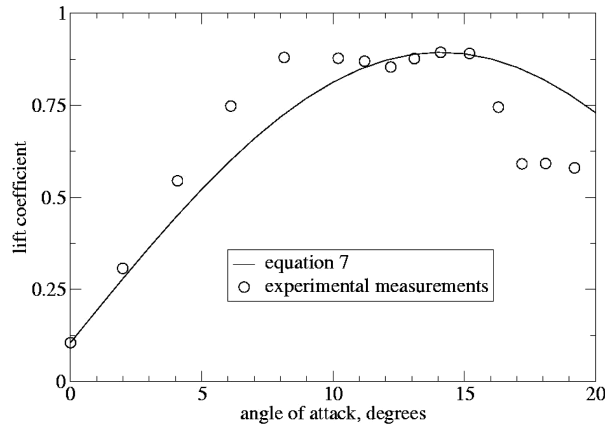Fig. 3 The chord width (taper) and pitch angle distribution along the span of the blade

Fig. 4 The lift curve slope for a section of the blade with the experimental values from Hand, *et al*. (2001), compared to the values produced by Eq. (7)

section (N.B. section 3 has an explanation of the approximations used for the lift coefficient for α values that occur outside this curve).

For each test, the wind turbine model is located in the centre of a computational domain made up of a three dimensional cube with 20 metre sides. The boundary conditions are uniform inflow, symmetry on the sides and a convective Orlansky condition at the outlet. In order to identify the effect of the velocity on the power generation, 16 different velocities between 5 and 20 metres per second are studied. These tests are repeated at three different grid resolutions with 30, 40 and 50 points in each direction. In each test the simulation lasted for 5 seconds which is enough time for the turbine to complete approximately 6 revolutions.

Fig. 5 shows that the power generated at low velocities is lower than the results for G and S. This is consistent with the observation of Xu and Sankar (2000) who observed that momentum theory combined with blade element theory (the theories used by G and S) tend to overestimate the power
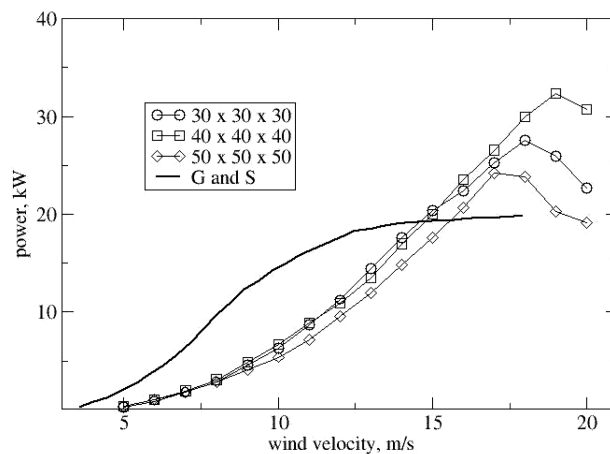

Fig. 5 The power produced against wind velocity. A comparison between the results of this model and those of Giguère and Selig (1999)
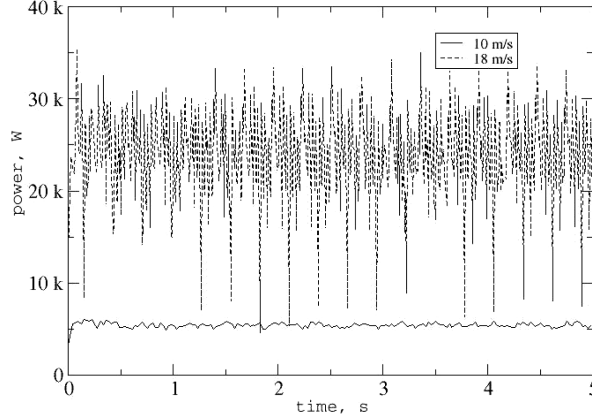
Fig. 6 The power produced with time at two different wind speeds with a $50 \times 50 \times 50$ grid

for low velocities.

Fig. 5 shows that there is some dependence of the power generated as a function of the resolution of the simulation. There are a wide range of factors which contribute to this.

The duration of the simulations of 5 seconds is perhaps not enough for full convergence of the results for each test. However Fig. 5 indicates that the solutions are stable even for the $18 \, \mathrm{m}^{-1}$ case (despite the scatter). The tests with higher velocities, in particular, show large oscillations in the power produced with time. The oscillations come mainly from the changes in the surface over which the forces are applied on the grid as the blades rotate. Further damping of the oscillations can come from inclusion of the drag force. Fig. 6 shows the power generated with time for velocities of 10 m/s and 18 m/s on a $50 \times 50 \times 50$ grid. For these higher velocities very large power changes are observed but this is because power is proportional to the cube of velocity so increases in the velocity strongly amplify any errors in how the forces are applied. This observation is similar to that seen in experiments where the values for the power generated at high velocities shows larger variation than that for lower velocities. It should also be noted that 18 m/s is at the upper performance limit for the wind turbine analysed here and most turbines automatically cut off when the wind speed goes beyond their upper design limit. Here the numerical error occurring has a more significant effect on the level of oscillation than that observed experimentally. Further comments are made in section 6 (ii).

5. Comparison with and without a tower and ground plane

The same turbine used in the previous section is studied with a grid of $30 \times 30 \times 30$ points and an inlet velocity of 15 m/s. Two simulations are carried out, one with a ground plane and a tower (with a diameter of 1.5 metres and a height of 10 metres) and a second without either the ground plane or the tower as for the previous section. The ground plane is modelled using a Werner Wengle (1991), power law for the wall shear stress. The Werner Wengle power law makes it possible to evaluate the surface friction velocity from a knowledge of velocity and position of the surface adjacent grid point

$$u_\tau = (B+1)\frac{(v)^B u_p}{[A(2y_n)^B]} + (1-B)\frac{(v)^{B+1} A^{(1+B)/(1-B)}}{[2(2y_n)^{B+1}]} \qquad (16)$$

where u_p is the velocity parallel to the surface, y_n is the normal distance to the velocity node and A and B are model constants $A = 8.3$, $B = 1/7$.

The tower is modelled as a simple cube with sides 1.5 m and a height of 10 m. Its surfaces are also modelled using the surface shear stress obtained from the Werner Wengle power law. In each test the simulation lasted 10 seconds after an initialisation period of 5 seconds.

In all cases no extra grid refinement was added to resolve the near wall boundary layers. This sort approach can be considered detrimental however, as Piomelli and Balaras (2002) discuss, the wall law can potentially fail if the grid is too refined.

The inlet flow field is kept uniform even for the case with a ground plane. This means that the inlet does not have a boundary layer profile and the boundary layer must develop within the domain. Since the Reynolds number (based on the turbine diameter and inlet velocity range between $5 \text{ ms}^{-1} < u < 20 \text{ ms}^{-1}$) of this problem varies between $4.2 \times 10^6 < Re < 16 \times 10^6$ it is envisaged that a turbulent wall boundary layer will develop very quickly in front of the inlet.

The non-dimensional wall height is of the order of $y^+ > 14000$ where $y^+ = u_\tau y / v$ with the friction velocity obtained from Eq. (16) using a near wall velocity of $u = 5 \text{ ms}^{-1}$ and grid size of 1.5 m. From this calculation it can be seen that the first grid point is still in the logarithmic region even at low near wall velocities.

An interesting characteristic has been studied in some detail in analyses of helicopter blade rotation (such as Kini and Conlisk 2002, Leishman, *et al.* 2002 and Kim, *et al.* 2002). This is the behaviour of the blade tip vortex. One good flow property for detecting the presence of vortices is the Q criterion, Dubief and Delcayre (2000). Positive values Q criterion, $Q = -1/4(\partial u_i/\partial x_j)(\partial u_j/\partial x_i)$, correspond to the centres of vortices. This quantity is more selective than total vorticity in locating vortices and is more easily extracted than local pressure minima.

Fig. 7 shows the effect of the tower on the Q criterion. The tip vortex seen clearly in the case without a ground plane or tower is destroyed. This figure also shows that the flow upstream of the tower is strongly affected by the presence of the tower. This is because the tower is surface is a rather poorly resolved square cylinder and hence has very strong blockage effects.
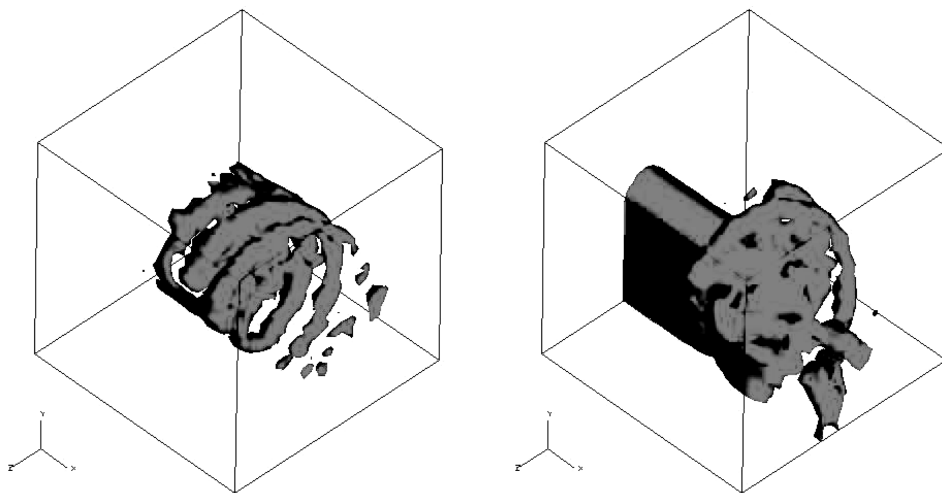

Fig. 7 The case with and without a tower with the Q criterion at $Q = 0.125$. The flow direction is in the positive x direction

The tower resolution needs to be finer because it acts as a bluff body causing the flow to be strongly distorted from equilibrium. Boundary layer laws (such as Werner and Wengle 1991, which is used for the ground plane) do not work properly. The results show considerable upstream as well as downstream effects. The level of the upstream effect gives an indication of how poorly the tower is resolved. This problem can be fixed by using finer resolution however, at the Reynolds numbers involved, this could become prohibitively expensive. Another far more attractive solution would be to treat the tower as a circular cylinder and apply circular cylinder lift and drag point forces in a similar manner to the way the turbine blades are modelled. This would then avoid the need of resolving the tower surface boundary layer and provide a good engineering representation of the effect of the tower on the flow field.

Fig. 8 shows mean velocity and axial velocity fluctuation profiles in front, behind and at the sides of the turbine. All the profiles are located along the centerline of the domain. The streamwise x positions represent the distance in front of the inlet. The centre of the tower is located at $x=8.5$ m. The figure
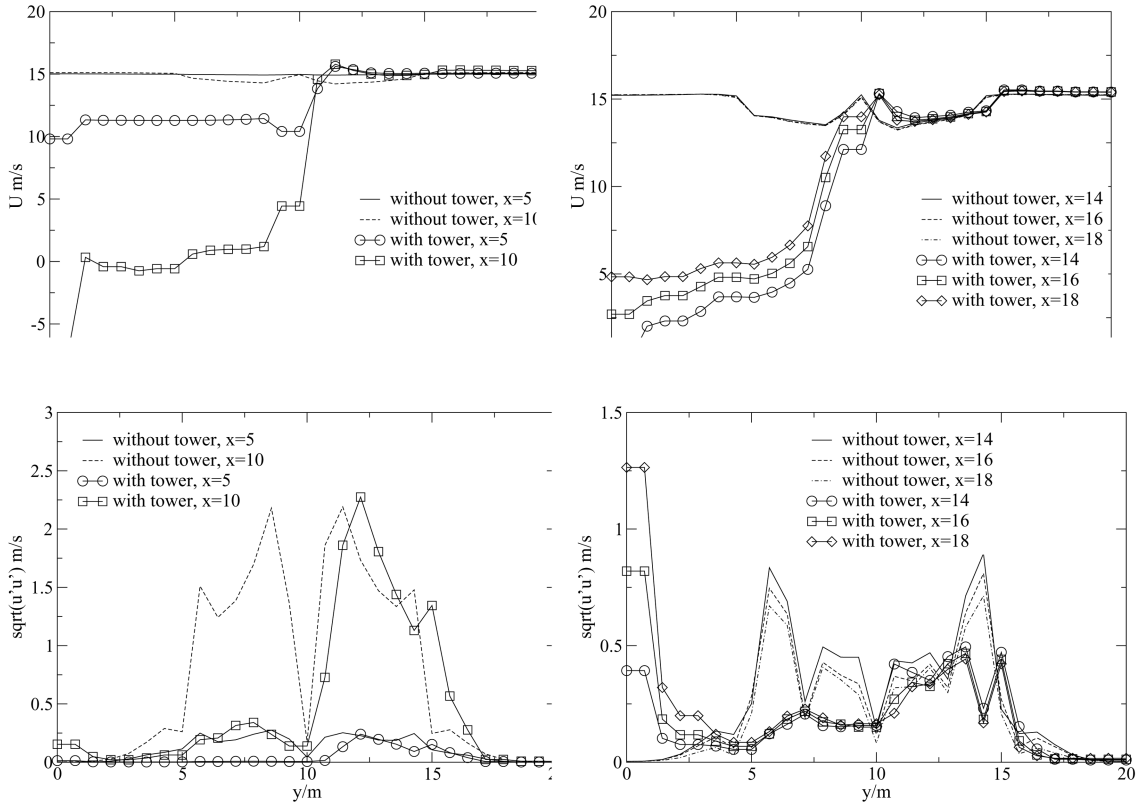

Fig. 8 The top two plots show mean velocity profiles and the bottom two plots show root mean square velocity fluctuation profiles at the spanwise centre of the domain ($z=10$ m). The profiles go from the ground plane or bottom boundary of the domain ($y=0$ m) to the upper boundary ($y=20$ m). The turbine hub is located at $x=8.5$ m, $y=10$ m, $z=10$ m and the blades, which have radii of just over 5 m, rotate in the $z-y$ plane. The left hand plots show profiles upstream ($x=5$ m) and immediately downstream ($x=10$ m) of the turbine. The right hand plots show profiles in the wake region further downstream $x=14$ m; 16 m; 18 m. Profiles with symbols correspond to the cases with the tower and ground plane included.

shows that the velocity in front ($x=5$ m) of the tower is strongly affected by it. A part of the flow which passes at $x=10$ m is blocked by the tower and the velocity is very small. In this region the flow near the ground is negative due to local recirculation. The tower creates a wake with a large reduction in the momentum and the velocities immediately in the wake at $x=14$, 16 and 18 are very reduced.

The boundary layer thickness at $x=5$ m in front of the inlet can be estimated from the small dip in the velocity profile near $y=0$ (shown by the circle symbols in the top left graph of Fig. 8). The boundary layer thickness near the outlet can be estimated from the high velocity fluctuation values on the profile near $y=0$ at $x=18$ m (shown by the diamond symbols in the bottom right graph of Fig. 8). These profiles indicate that the boundary layer thickness does not grow significantly along the length of the domain.

As discussed, Fig. 8 shows that the tower obstructs the flow turbulence in front of the turbine. The same figure shows that behind the tower at the stations $x=14$, 16 and 18 the turbulence in the region above the tower (10 m$<y<$20 m) is also reduced. This is because the tower inhibits the generation of the tip vortex. These profiles also show the development of a turbulent boundary layer near the ground plane. Improvements to this type of approach are given in the discussion and further work section.

The power production remains largely unchanged between the two cases. Fig. 8 shows that the flow immediately behind the tower is reduced however the flow immediately above the tower is increased. This is also true for the flow either side of the tower. This means that the power production when a blade is directly behind the tower is decreased but when a blade passes either side of the tower the power production is slightly increased. The overall effect is that the power does not really change due to the tower for this simplified case.

Fig. 9 shows the pressure field just behind the rear surface of the tower at three consecutive instants in time. This figure shows that as the blades pass the tower, the tower surface experiences increases in local pressure where the main power generating 16 part of the blade passes. This oscillating forcing has implications for the long term fatigue loading on the tower structure.

The tower and ground plane are included without change to the grid. At first sight this might appear a rather crude approach. However, in order to treat practical applications, coarse grids must be used. Methods must be developed and tested with this in mind. These results are presented as an indication of the types of difficulties that can be encountered.
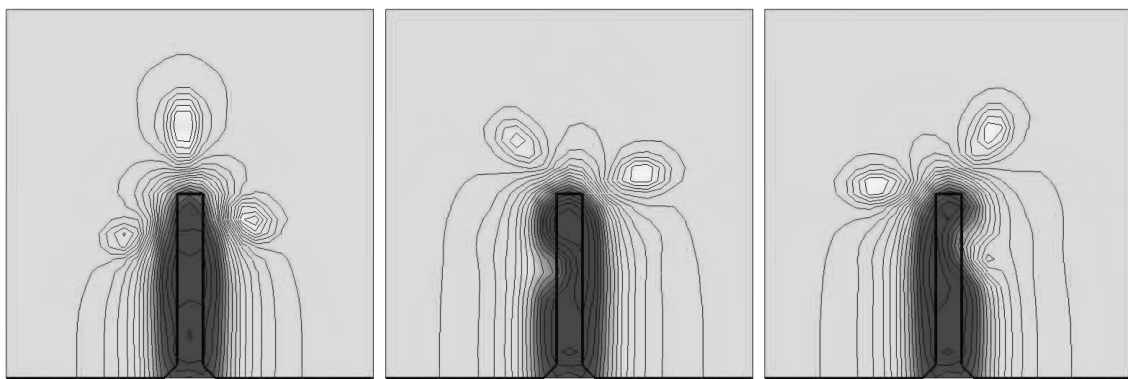

Fig. 9 The pressure field just behind the tower at three consecutive 0.1 second intervals. Blue represents low pressure and red/yellow high pressure. The high pressure regions correspond to the main power generating regions of the turbine where the lift forces are larger and the low pressure regions correspond to the immediate wake behind the tower

6. Discussion and further work

Since it makes use of blade element theory, the approach for modelling the rotating blades used here, does not require resolution of individual blade surfaces unlike Johansen, *et al.* (2002). This avoids the necessity for very fine meshes in the blade regions - although the mesh must be dense enough to model the full length of the blade. The model can be applied within any coordinate system. Thus it is possible to include the model within simulations using non-structured meshes over complex terrain with several turbines operating at the same time.

A major problem in this study is the rather over simplified representation of blade element theory. There are several improvements that must be made to exploit the full physical basis of blade element theory and its application to wind turbine aerodynamics: (i) A more complete model should include the torque and hence drag force on each blade element as these will have important effects on the local flow. In addition the torque is the force that the flow applies to the turbine leading to a power production therefore it should be included to capture the full physics of the problem. (ii) As the blades are rotated, the relative distances between the locations of the point forces and the centres of the grid elements where the point forces applied are not taken into account. Thus, the point forces effectively act at the element centres. This contributes to the scattered high frequency behaviour of the subsequent power output. The actual locations of the point forces within each grid must be taken into account and further tests need to be done to ensure improvements do not cause grid dependency. (iii) A vortex produced at the tip of the rotating blades reduces the lift coefficient to below that predicted by blade element theory over the outermost tip region of the blade. This tip loss behaviour must be added to modify the basic blade element theory for rotating blades. (iv) The centrifugal force along the rotating blades acts to convect stalled air away from the blade root. This skewing of the boundary layer delays the separation that would otherwise be predicted for 2D blade element theory. This stall delay effect should also be included.

The rotational forcing will be damped by inclusion of the drag force, (i), and the high frequency oscillations will be reduced by a more balanced application of the blade forces as they rotate, (ii). Tip loss, (iii), and stall delay, (iv), effects will act to improve the way the main power generating parts of the blades are modelled. Modifications for tip loss are normally to convert the two dimensional standard blade element lift coefficient, $c_{l_{2D}}$, to include the three dimensional effects therefore becoming $c_{l_{3D}}$. A suggested tip loss model from Xu and Sankar (2002), is

$$c_{l_{3D}} = F c_{l_{2D}} \tag{17}$$

where $F = 0.8$ when $r/R > 0.8$ and $F = 1$ when $r/R < 0.8$ where r is the radial location of the blade element and R is the radius of the blade. A suggested stall delay model also from Xu and Sankar (2002), is

$$c_{l_{3D}} = c_{l_{2D}} + \alpha \Delta \alpha \tag{18}$$

where α is the slope of the linear part of the c_l/α curve and

$$\Delta \alpha = (\alpha_{c_{l_{\max}}} - \alpha_{c_{l_0}}) \left(\frac{c/r}{0.136} \left[\frac{c/r}{0.1517} \right]^{-1/1.084} - 1 \right)$$

with c the local chord. Further details on tip loss and stall delay models are given in Xu and Sankar (2002). The lift curve slope could also be made to more closely fit the experimental data. Additional development of the approach used in this paper should address all of these points.

The tower model used is also rather simple and assumes the tower has a square cross-section. This accounts for the poorly resolved tower surface resolution and hence large blockage effects. A far better way to model the tower would be as a line of stationary point forces in a similar way to the blades except that the tower could make use of the lift and drag properties of a standard circular cylinder. This would avoid the necessity of dense grids to resolve the tower surface.

The simulations involving the ground plane and tower help to highlight the fact that the grids used for this study are not fitted to the turbine. This is the case in the vast majority of wind turbine simulations. Rotating the blade forcing within the grid incurs problems such as those discussed in point (ii) above. However the approach can extend the potential application of the model to realistic practical situations.

7. Conclusions

A three dimensional non-stationary model for simulating the transient characteristics of the wake behind a wind turbine is proposed for an LES. Information for the blade geometric and aerodynamic characteristics is applied and showed that the model could produce a power curve with a broadly similar behaviour to that produced by other studies. The simulation showed physical characteristics of the flow such as the tip vortex. This type of feature cannot be observed using the majority of approaches used to analyse wind turbines.

The effects of the ground plane and a tower on the flow around a wind turbine are studied. It was observed that the the flow in front of the turbine was affected and the tower itself generated a wake which was responsible for the destruction of the blade tip vortex. The pressure field on the rear of the tower showed that the tower experienced periodic unsteady loading as the blades passed.

Both the turbine blade and tower models used are rather over simplified. Improvements have been proposed to obtain a more realistic representation of the wind turbine and tower flowfields. For instance the effect of the torque must be included in the turbine model and the tower could be modelled as point aerodynamic forces from a circular cylinder.

Acknowledgements

References

Ackermann, C. (2000), "Développements et validation de simulation des grandes echelles d'écoulements turbulents dans un code industriel", PhD thesis, Institut National Polytechnique de Grenoble, France, December.
Ammara, I., Leclerc, C. and Masson, M. (2002), "A viscous three-dimensional differential/actuator-disk method for the aerodynamic analysis of wind farms", *J. Solar Eng.*, ASME, **124**, 345-356.
Barthelmie, R. J. (Ed.) (2002), "Offshore wakes: measurements and modelling", *Proceeding of the ENDOW workshop*, Riso-R-1326(EN), Riso National Laboratory, Roskilde, Denmark, March.
Bindner, H. (1999), "Power control for wind turbines in weak grids", Risoe-R-1117(EN), Risoe National

Laboratory, Roskilde, Denmark, March.

Dubief Y. and Delcayre, F. (2000), "Coherent-vortex identification in turbulence", Institute of Physics Publishing Ltd, *J. Turbulence*, **1**(11).

Emonot, P. (1992), "Méthodes de volumes elénts finis: application aux equations de Navier-Stokes et résultas de convergence", PhD thesis, Université Claude Bernard Lyon I.

Giguère, P. and Selig, M. S. (1999), "Design of a tapered and twisted blade for the NREL combined experimental rotor", NREL/SR-500-26173, National Renewable Energy Laboratory, U.S. Department of Energy, April.

Hand, M. M., Simms, D. A., Fingersh, L. J., Jager, D. W., Cotrell, J. R., Schreck, S. and Larwood, S. M. (2001), "Unsteady aerodynamics experiment Phase IV: Wind tunnel test configurations and available data configurations", NREL/TP-500-29955, National Renewable Energy Laboratory, U.S. Department of Energy, December.

Hahm, T. and Kröning, J. (2001), "3D simulation of the wake of a wind turbine", *Deutsche Windenergie-Institut Magazin*, nr 18, February.

Howard, R. J. A. and Pereira, J. C. F. (2003), "Modelo de aerogeradores para o cálculo das grandes escalas", *VII Cong. de Mecânica e Computational*, University of Evora, April 2003, pp1177-1186, ISBN 972-778-058-X.

Howard, R. J. A. and Pourquié, M. (2002), "Large eddy simulation of an Ahmed reference model", *J. Turbulence*, **3**, 012, Institute of Physics pub. Ltd.

Johansen, J., Sorensen, N., Michelsen, J. and Schreck, S. (2002), "Detached eddy simulation of flow around the NREL Phase VI blade", *Wind Energy*, **5**(2/3), 185-197.

Jonkman, J. M. (2003), "Modeling of the UAE wind turbine for refinement of FAST AD", NREL/TP-500-34755, National Renewable Energy Laboratory, U.S. Department of Energy, December.

Källstrand, B., Bergström, H., Hojstrup, J. and Smedman, A. (2000), "Mesoscale wind field modifications over the Baltic sea", *Boundary Layer Meteorology*, **95**, 161-188, Kluwer. 21.

Kim, H., Williams, H. and Lyrintzis, A. S. (2002), "Improved method for rotor wake capturing", *AIAA, J. Aircraft*, **39**(5), 794-803, September-October.

Kini, S. and Conlisk, A. T. (2002), "Nature of locally steady rotor wakes", *AIAA, J. Aircraft*, **39**(5), 750-758, September-October.

Leishman, J. G., Bhagwat, M. J. and Bagai, A. (2002), "Free-vortex filament methods for the analysis of helicopter rotor wake", *AIAA, J. Aircraft*, **39**(5), 759-775, September-October.

Masson, M., Smaili, A. and Leclerc, C. (2001), "Aerodynamics analysis of HAWTs operating in unsteady conditions", *Wind Energy*, **4**, 1-22.

Piomelli, U. and Balaras, E. (2002), "Wall-layer models for large eddy simulations", *Ann. Rev. Fluid Mech.*, **34**, 349-374.

Sagaut, P. (2004), *Large eddy simulation for incompressible flows. An introduction*, Springer, Scientific Computing, ISBN 1434-8322.

Snel, H. (1998), "Review of the present status of rotor aerodynamics", *Wind Energy*, **1**, 49-69.

Sorensen, N., Michelsen, J. and Schreck, S. (2002), "Navier-stokes predictions of the NREL phase VI rotor in the NASA Ames 80ft × 120ft wind tunnel", *Wind Energy*, **5**(2/3), 151-169.

Sorensen, J. N. and Shen, W. Z. (2002), "Numerical modeling of wind turbine wakes", *J. Fluids Eng.*, ASME, **124**, 393-399.

Werner, H. and Wengle, H. (1991), "Large eddy simulation of turbulent flow over and around a cube in a plate channel", *8th Symposium on Turbulent Shear Flow*, Technical University of Munich, Germany, Sept 9-11.

Wood, D. (2002), "The design and analysis of small wind turbines", http://www.wind.newcastle.edu.au/notes.html, School of Engineering, University of Newcastle, NSW 2308, Australia.

Xu, G. and Sankar, L. N. (2000), "Computational study of horizontal axis wind turbines", *J. Solar Energy*, ASME, **122**, 35-39, February.

Xu, G. and Sankar, L.N. (2002), "Development of engineering aerodynamics models using a viscous flow methodology on the NREL Phase VI blade", *Wind Energy*, **5**(2/3), 171-183.

Yamaguchi, A., Ishihara, T. and Fujino, Y. (2003), "Experimental study of the wind flow in a coastal region of Japan", *J. Wind Eng. Ind. Aerodyn.*, **91**, 247-264, Elsevier.

GS